



Structure and Characterization of a Covalent Inhibitor of Src Kinase

Deepak Gurbani^{1†}, Guangyan Du^{2,3†}, Nathaniel J. Henning^{2,3†}, Suman Rao^{2,3,4}, Asim K. Bera¹, Tinghu Zhang^{2,3*}, Nathanael S. Gray^{2,3*} and Kenneth D. Westover^{1*‡}

OPEN ACCESS

Edited by:

Megha Agrawal,
University of Illinois at Chicago,
United States

Reviewed by:

Matthew Bryan Soellner,
University of Michigan, United States
Dustin Maly,
University of Washington,
United States
Ramya Sivakumar,
Fred Hutchinson Cancer Research
Center, United States

*Correspondence:

Nathanael S. Gray
nathanael_gray@dfci.harvard.edu
Tinghu Zhang
tinghu_zhang@dfci.harvard.edu
Kenneth D. Westover
kenneth.westover@utsouthwestern.edu

[†]These authors have contributed
equally to this work

[‡]Lead Contact

Specialty section:

This article was submitted to
Molecular Diagnostics and
Therapeutics,
a section of the journal
Frontiers in Molecular Biosciences

Received: 17 February 2020

Accepted: 08 April 2020

Published: 19 May 2020

Citation:

Gurbani D, Du G, Henning NJ, Rao S,
Bera AK, Zhang T, Gray NS and
Westover KD (2020) Structure and
Characterization of a Covalent Inhibitor
of Src Kinase. *Front. Mol. Biosci.* 7:81.
doi: 10.3389/fmolb.2020.00081

¹ Departments of Biochemistry and Radiation Oncology, The University of Texas Southwestern Medical Center at Dallas, Dallas, TX, United States, ² Department of Biological Chemistry and Molecular Pharmacology, Harvard Medical School, Boston, MA, United States, ³ Department of Cancer Biology, Dana Farber Cancer Institute, Boston, MA, United States, ⁴ Harvard Program in Therapeutic Science (HITS), Harvard Medical School, Boston, MA, United States

Unregulated Src activity promotes malignant processes in cancer, but no Src-directed targeted therapies are used clinically, possibly because early Src inhibitors produce off-target effects leading to toxicity. Improved selective Src inhibitors may enable Src-directed therapies. Previously, we reported an irreversible Src inhibitor, DGY-06-116, based on the hybridization of dasatinib and a promiscuous covalent kinase probe SM1-71. Here, we report biochemical and biophysical characterization of this compound. An x-ray co-crystal structure of DGY-06-116: Src shows a covalent interaction with the kinase p-loop and occupancy of the back hydrophobic kinase pocket, explaining its high potency, and selectivity. However, a reversible analog also shows similar potency. Kinetic analysis shows a slow inactivation rate compared to other clinically approved covalent kinase inhibitors, consistent with a need for p-loop movement prior to covalent bond formation. Overall, these results suggest that a strong reversible interaction is required to allow sufficient time for the covalent reaction to occur. Further optimization of the covalent linker may improve the kinetics of covalent bond formation.

Keywords: src kinase, cancer, dasatinib, selectivity, irreversible inhibitor

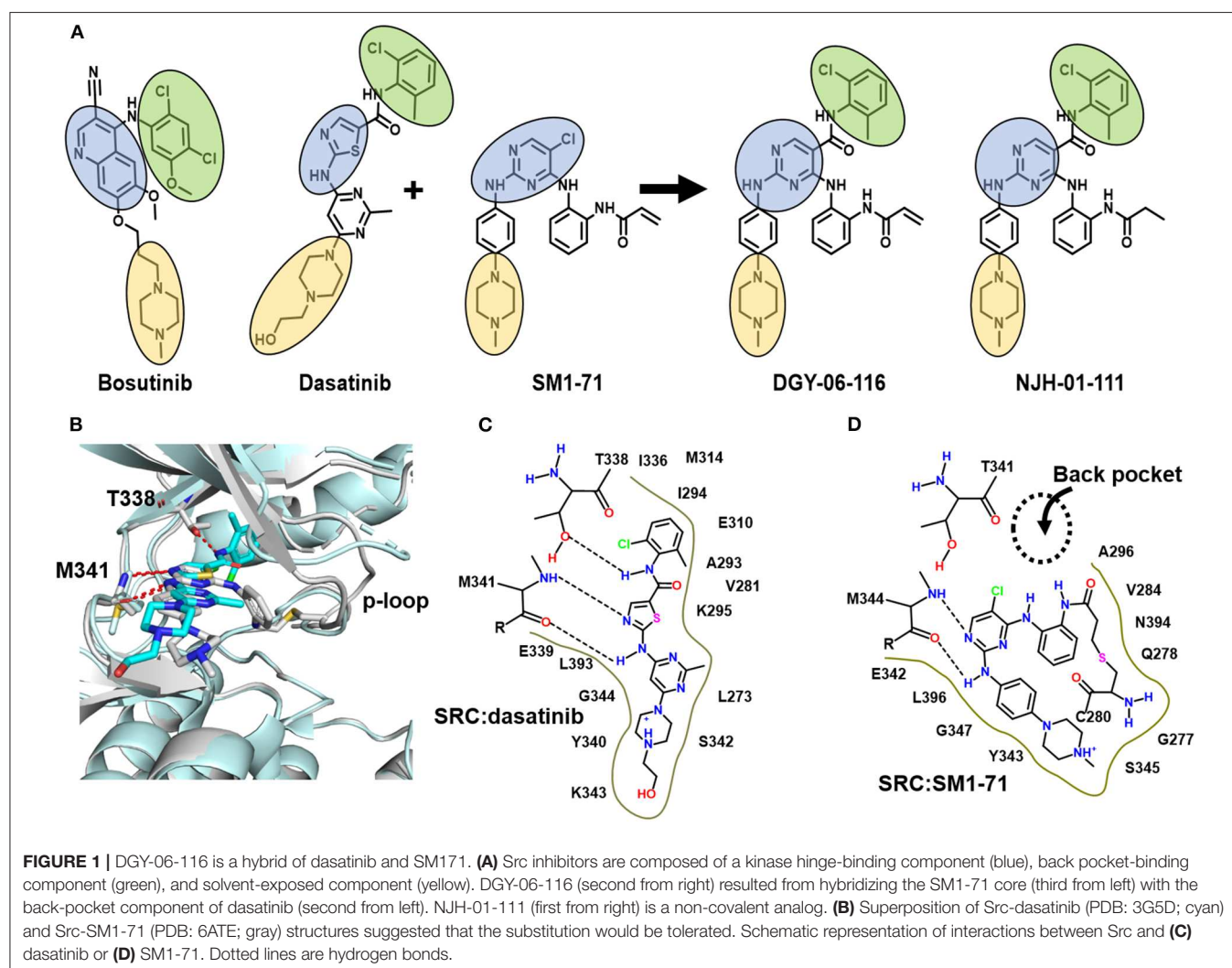
INTRODUCTION

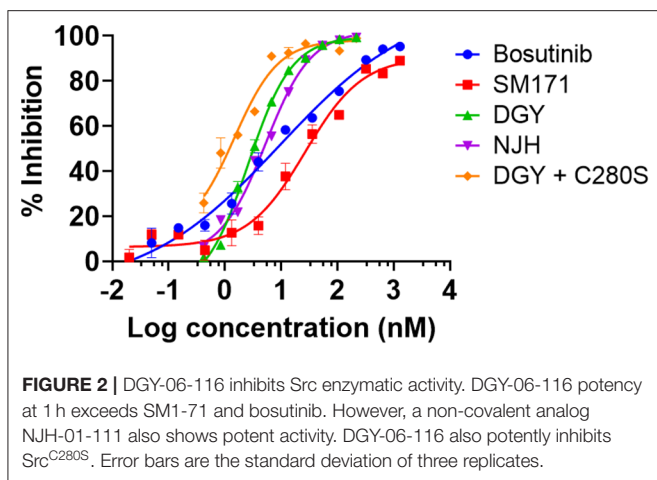
SRC was among the first oncogenes to be discovered (Stehelin et al., 1976) and encodes a non-receptor protein tyrosine kinase that regulates many cancer-related cellular processes including mitogenesis, angiogenesis, adhesion, invasion, migration, and survival (Sen and Johnson, 2011). Src activity drives malignant phenotypes in hematologic and solid cancers including breast, prostate, lung, colorectal, and pancreatic cancer (Araujo and Logothetis, 2010; de Felice et al., 2016; Appel et al., 2017). Genetic ablation of Src in animal models reverses cancer phenotypes without systemic toxicity (Trevino et al., 2006; Ammer et al., 2009; Marcotte et al., 2012), suggesting that Src inhibition may be effective in treating certain cancers (Araujo and Logothetis, 2009; Zhang et al., 2009; Chen et al., 2014; Anderson et al., 2017; Appel et al., 2017). Src has also been implicated in cancer drug resistance (Carretero et al., 2010; Sen et al., 2011). Nevertheless, selective Src inhibition has not been demonstrated as a driver of efficacy for any of the clinically used multi-targeted Src drugs.

Dasatinib and bosutinib inhibit multiple kinases including Src, but are approved as anti-Bcr-Abl therapies to treat chronic myelogenous leukemia and acute lymphoblastic leukemia (Shah et al., 2010; Keskin et al., 2016; Cortes et al., 2019). Src-directed trials using dasatinib failed in part due to dose-limiting toxicity (Araujo and Logothetis, 2010; Algazi et al., 2012; Araujo et al., 2012; Secord et al., 2012; Sharma et al., 2012; Schott et al., 2016) including grade 3 to 4 diarrhea, thrombocytopenia, neutropenia, and anemia (Buglio et al., 2012; Daud et al., 2012). These toxicities may be due to the multi-targeted nature of these compounds that also inhibit members of the Src family of kinases (SFKs), Bcr-Abl, c-Kit, PDGFR, c-Fms, and EphA2. Improved Src inhibitors with better selectivity may enable Src-directed cancer therapies.

Engineering selectivity into Src inhibitors is challenging because of the high degree of sequence homology between Src family members and other receptor tyrosine kinases (Duan et al., 2014; Elias and Ditzel, 2015). One strategy for achieving selectivity in kinases is to utilize covalent chemistry, targeting non-conserved cysteines near the inhibitor

binding site. Prior work showed that Src, in particular, is amenable to this approach by targeting non-conserved cysteines in the p-loop (Kwarcinski et al., 2012). In that work, promiscuous scaffolds, including the dasatinib scaffold, were derivatized to include reactive warheads that could react with p-loop cysteines, resulting in enhanced selectivity for kinases that include a p-loop cysteine. The work generated hypotheses regarding the importance of p-loop dynamics for this class of inhibitor, but structural data were not reported. Recently, we found an opportunity to build upon this strategy when we found that SM1-71, a 2, 4-disubstituted pyrimidine that includes a cysteine-reactive warhead, can covalently modify 23 different kinases including Src. Our Src-SM1-71 crystal structure (PDB: 6ATE) revealed the Src p-loop in a kinked conformation (Rao et al., 2019). We subsequently showed that SM-1-71 could be optimized for Src inhibition by hybridization with dasatinib (Figures 1A–D, Figure S1; Du et al., 2020). Here, we present formal biochemical, biophysical, and structural characterization of Src inhibition by DGY-06-116.





RESULTS

DGY-06-116 Potently Inhibits Src Kinase Activity

DGY-06-116 was previously characterized for the ability to bind Src (Du et al., 2020). Here, we evaluated the relative potency of inhibitors on Src enzymatic activity using a mobility shift assay (MSA), which measures phosphorylation of a peptide substrate of Src. Given that covalent inhibitors can show time-dependent effects on IC_{50} values, we use a 1-h time point for all samples so relative potencies are comparable. At 1-h incubation, DGY-06-116 showed an IC_{50} , 1 h of 2.6 nM. This was substantially better than SM1-71 (IC_{50} , 1 h of 26.6 nM), bosutinib (IC_{50} of 9.5 nM), and its non-covalent analog NJH-01-111 (IC_{50} of 5.3 nM) (Figure 2). To estimate the contribution of covalent binding to the overall potency of DGY-06-116, we also tested Src^{C280S}, which cannot form a covalent bond because of the cysteine-to-serine mutation. Src^{C280S} showed excellent kinase activity, although specific activity was less (~50%) than that of wild-type protein (Figure S2B). DGY-06-116 showed comparable IC_{50} , 1 h values for mutant and wild-type Src (Figure 2), suggesting that reversible binding substantially contributes to the potency of this compound. To confirm this, we also tested a non-covalent analog of DGY-06-116, NJH-01-111, in which the acrylamide warhead is replaced with propionamide (Figure 1A). The IC_{50} of NJH-01-111 could not be distinguished from DGY-06-116, confirming that the core scaffold supports the potency of this compound class (Figure 2).

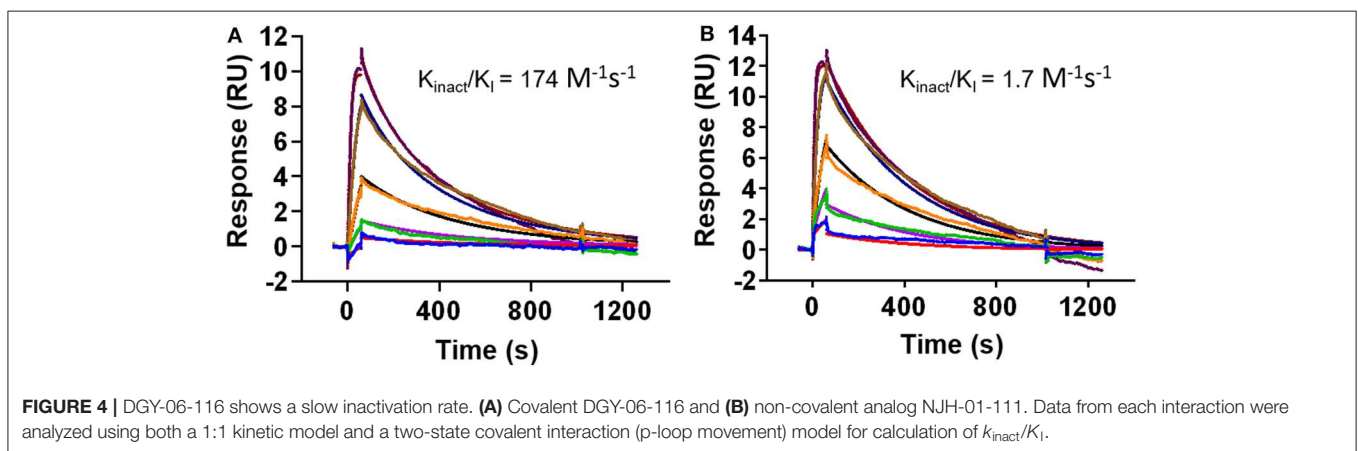
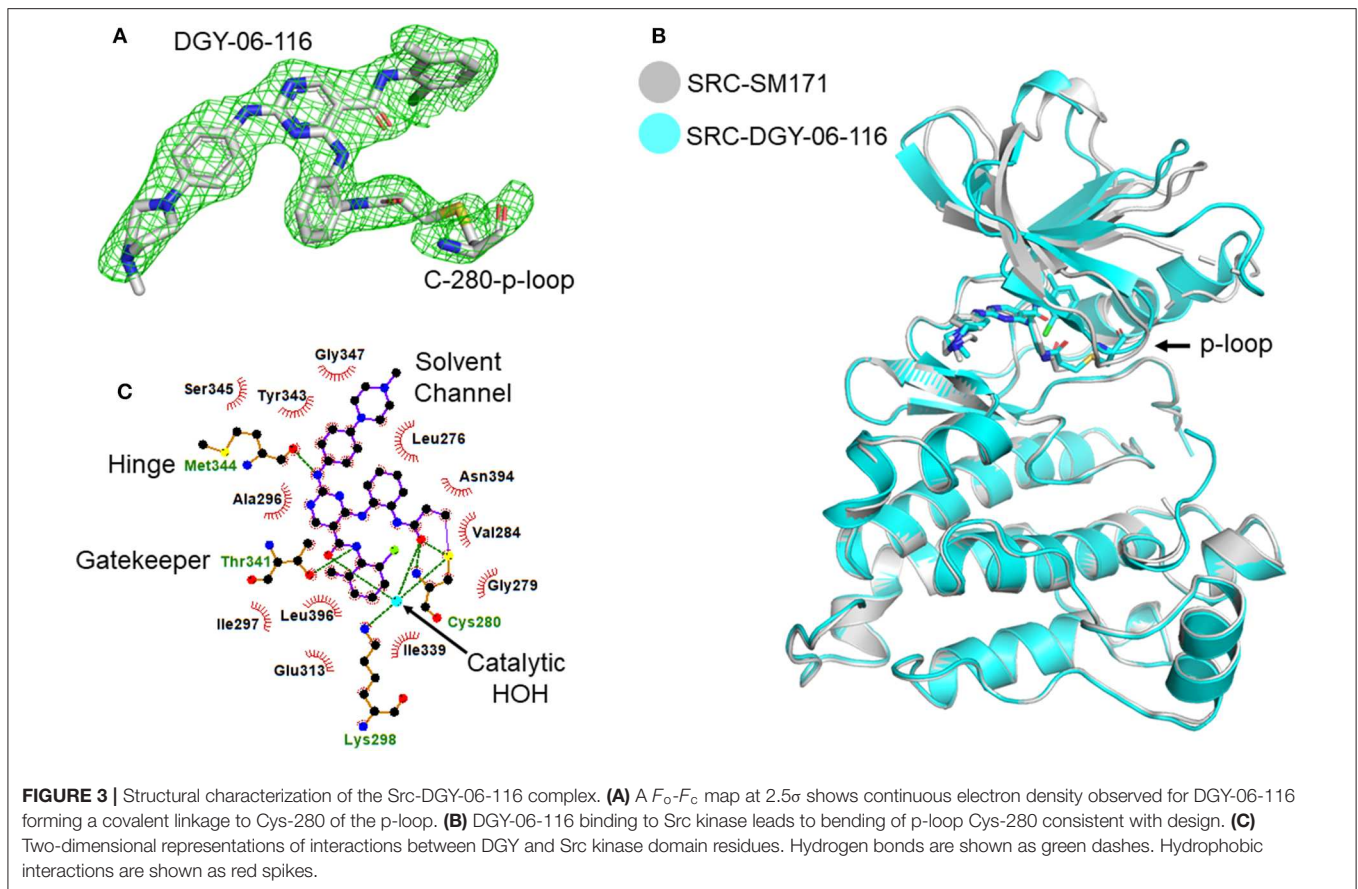
Structure of the Src-DGY-06-116 Complex

To further understand the nature of the interactions between DGY-06-116 and Src, we determined a co-crystal structure of DGY-06-116 with Src (PDB code: 6E6E) at 2.15 Å resolution. Data collection and refinement statistics are shown in Table 1. This structure includes eight molecules in the asymmetric unit. The main difference between individual protomers was variation in an N-terminal lobe loop conformation, but there were no differences in the conformations of the ATP binding sites (Figure S3). DGY-06-116 was easily modeled into the predicted

TABLE 1 | Data collection and refinement statistics.

Crystallography statistics	
DATA COLLECTION	
X-ray source	APS 19-1D
Wavelength (Å)	0.9795
Space group	P1
Unit cell	
a, b, c (Å)	63.53, 84.03, 120.11
α , β , γ (°)	89.96, 90.05, 90.12
Resolution (Å)	50.00–2.15 (2.19–2.15) a
Unique reflections	123,213
Redundancy	3.6 (3.0)
Completeness (%)	91.7 (91.6)
Wilson B-factor	32.1
R_{merge} (%)	12.7 (96.4)
I/σ	9.7 (1.0)
REFINEMENT	
Resolution	43.66–2.15 (2.19–2.15)
Reflections Used	122,649
R_{free} reflections	5,955
$R_{\text{work}}/R_{\text{free}}$ (%)	25.0/28.5
Non-hydrogen atoms	17,919
Protein	17,140
Water	435
Ligand	344
RMSD	
Bond lengths (Å)	0.002
Bond angles (°)	0.592
Average B-factor (Å ²)	46
Protein	46.84
Ligands	31.75
Water	38.46
Ramachandran plot (%)	
Favored	95.02
Allowed	4.11
Disallowed	0.4
PDB accession code	6E6E

binding site for all, with the warhead forming continuous electron density with Cys-280 (Figure 3A). As seen with SM171, the p-loop of the Src kinase is bent and thus allows a covalent bond to form, a phenomenon that is not observed with other Src structures (Figure 3B). As expected, the nitrogen of DGY-06-116's carboxamide linker hydrogen bonds to gatekeeper Thr-338. The nitrogen is also part of a coordinated hydrogen bonding network that includes an active-site water (HOH432), catalytic Lys-298, the backbone of Cys-280, and the carbonyl DGY-06-116 (Figure 3C). The chloro-methyl phenyl substituent is situated in the back pocket of the Src kinase, creating hydrophobic interactions with Ile-297 and Leu-396. The anilino-pyrimidine forms two hydrogen bonds with the backbone of Met-341 in the hinge region and the methyl piperazinyl tail extends to



the solvent channel forming hydrophobic contacts with Val-284 and Gly-347 (**Figure 3C**). These results confirm that DGY-06-116 forms a covalent bond with Cys-280, but also suggest that hydrophobic interactions with the back pocket significantly contribute to affinity, possibly explaining the high potency of the non-covalent analog NJH-01-111.

Inactivation by Src by DGY-06-116 Is Slow

While the crystal structure clearly indicates covalent binding to Src, the enzymatic assay could not distinguish between

DGY-06-116 and NJH-01-111. Nevertheless, clear differences are seen in the selectivity of these compounds (Du et al., 2020). Previously, we used the MSA to measure the inactivation rate of other covalent inhibitors (Tan et al., 2017). However, in this case, we could not because the IC_{50} , 1 h of for DGY-06-116 was near the enzyme concentration used in the assay and therefore close to the theoretical sensitivity limit. To evaluate the inactivation rate, we used a surface plasmon resonance assay to estimate k_{inact}/K_I (Copeland, 2013; Miyahisa et al., 2015). In our setup, biotinylated Src kinase was immobilized on the

biosensor. Binding kinetics for DGY-06-116 and NJH-01-111 were found to be similar, indicating a similar initial binding event (Figures 4A,B). Although the decay appeared similar on visual inspection, we were unable to fit the curve for DGY using a one-state model. We considered that the p-loop must move into position to allow a covalent bond to form. We therefore used a two-state model to calculate k_{inact}/K_I . For the non-covalent inhibitor NJH-01-111, the value was only $1.7 \text{ M}^{-1} \text{ s}^{-1}$, indicating that a covalent bond did not form. In contrast, k_{inact}/K_I for DGY-06-116 was $174 \text{ M}^{-1} \text{ s}^{-1}$, consistent with covalent bond formation. However, when comparing inactivation rate constant (k_{inact}), DGY-06-116 showed a rate of $5.7 \times 10^{-7} \text{ s}^{-1}$, several orders of magnitude slower than for other validated covalent compounds such as neratinib ($2 \times 10^{-3} \text{ s}^{-1}$) and afatinib ($1 \times 10^{-3} \text{ s}^{-1}$) (Gierse et al., 1999; Papp-Wallace et al., 2014; Schwartz et al., 2014), showing modest irreversible inhibition. Given that the p-loop must shift to form a covalent bond with DGY-06-116, we speculate that this slow k_{inact} occurs because it depends on protein dynamics at the p-loop. This is in agreement with prior ideas about the importance of p-loop movement for p-loop targeted inhibitors (Kwarcinski et al., 2012).

DISCUSSION

In these studies, we established that DGY-06-116 binds covalently to Src in a manner similar to SM1-71, where the p-loop must kink to establish the covalent bond. However, we also showed that a non-covalent analog, NJH-01-111, binds with a similar high affinity. We also showed that the covalent reaction is slow. Altogether, our interpretation of these findings is that a strong reversible interaction is required to allow sufficient time for the p-loop to sample a kinked conformation compatible with covalent bond formation.

We speculate that that optimization of the interaction between the p-loop and compound may increase the inactivation rate, leading to further improvements in compound selectivity in biological systems, since covalent bond formation appears to be the major driver of selectivity (Du et al., 2020). One way to do this would be to increase the length of the linker to the covalent warhead so the p-loop does not have to kink. Computationally, this appears to be a viable strategy since simulated docking shows that extended linkers retain existing interactions and may even add additional hydrogen bonding with the main-chain oxygen of Gln-275 (Figure S4).

Despite the slow inactivation rate of DGY-06-116, this compound is a selective Src inhibitor that will enable laboratory studies of Src-driven biology, with applications in cancer. One potential application may relate to the subject of acquired resistance, which is a major challenge with kinase inhibitors (Lovly and Shaw, 2014). Src has been implicated in mechanisms that underlie the development of hormone therapy resistance in breast cancer (McDonnell and Norris, 2002; Hiscox et al., 2006) and resistance to chemotherapy in triple-negative breast cancer (Wu et al., 2016). Src is also involved in drug resistance to Her2-directed therapy and for certain head and neck and lung cancers (Carretero et al., 2010; Sen et al., 2011). Src has

also been implicated in non-small cell lung cancers harboring mutations in EGFR where Src is activated via Cripto-1 (Park et al., 2014). Indeed, this concept is being tested in a clinical trial (NCT02954523) where dasatinib and osimertinib are delivered together. Another possible application is in KRAS-mutated lung cancer, where loss of the Lkb1 tumor suppressor activates Src signaling. In mouse cancer models that mimic this cancer state, the combined inhibition of Src, PI3K, and Mek showed synergistic tumor regression (Carretero et al., 2010). Finally, a lack of predictive biomarkers has limited prior Src-directed trials (Puls et al., 2011). Our tool compound may allow us to identify cancer populations that are sensitive to Src inhibition through chemistry-first biomarker discovery approaches (McMillan et al., 2018).

ACCESSION CODES

The atomic coordinates and structure factors have been deposited in the RCSB Protein Data Bank archive (PDB) for human proto-oncogene tyrosine-protein kinase Src in complex with DGY-06-116 (PDB ID: 6E6E). SRC_HUMAN P12931.

DATA AVAILABILITY STATEMENT

This article contains previously unpublished data. The name of the repository and accession number(s) are not available.

AUTHOR CONTRIBUTIONS

NG, TZ, KW, and DG: Conceptualization. GD and NH: Chemistry. DG: Structure determination and biochemistry. TZ, DG, KW, and NG: Writing. The manuscript was edited through contributions of all authors. All authors have given approval to the final version of the manuscript.

FUNDING

This work was supported by Welch I-1829, ACS RSG-18-039-01-DMC, and a Career Enhancement Grant through NIH P50CA07090720 to KW and by Linde Center for medicinal chemistry to NG.

ACKNOWLEDGMENTS

Results shown in this report are derived from work performed at Argonne National Laboratory, Structural Biology Center (SBC) at the Advanced Photon Source. SBC-CAT is operated by UChicago Argonne, LLC, for the U.S. Department of Energy, Office of Biological and Environmental Research under contract DE-AC02-06CH11357. We thank Eric Roush for technical assistance with the Biacore S200 instrument and data analysis. We also thank Dr. Damiana Chiavolini for editing the manuscript.

SUPPLEMENTARY MATERIAL

The Supplementary Material for this article can be found online at: <https://www.frontiersin.org/articles/10.3389/fmolb.2020.00081/full#supplementary-material>

Figure S1 | Src kinase domain architecture and location of targetable cysteine the p-loop.

Figure S2 | Src^{C280S} efficiently phosphorylates the peptide substrate. Percent conversion from non-phosphorylated to phosphorylated substrate is shown over time for a range of Src concentrations. Each data point represents a triplicate measurement. **(A)** WT Src. **(B)** Src^{C280S}.

Figure S3 | Differences between protomers in the asymmetric crystallographic unit. All 8 protomers were superimposed and each colored differently.

Figure S4 | Covalent docking model predicts hydrogen bonding interactions for linker optimization.

REFERENCES

- Adams, P. D., Afonine, P. V., Bunkoczi, G., Chen, V. B., Davis, I. W., Echols, N., et al. (2010). PHENIX: a comprehensive Python-based system for macromolecular structure solution. *Acta Crystallogr. D Biol. Crystallogr.* 66(Pt 2), 213–221. doi: 10.1107/S0907444909052925
- Algazi, A. P., Weber, J. S., Andrews, S. C., Urbas, P., Munster, P. N., DeConti, R. C., et al. (2012). Phase I clinical trial of the Src inhibitor dasatinib with dacarbazine in metastatic melanoma. *Br. J. Cancer* 106, 85–91. doi: 10.1038/bjc.2011.514
- Ammer, A. G., Kelley, L. C., Hayes, K. E., Evans, J. V., Lopez-Skinner, L. A., Martin, K. H., et al. (2009). Saracatinib impairs head and neck squamous cell carcinoma invasion by disrupting invadopodia function. *J. Cancer Sci. Ther.* 1, 52–61. doi: 10.4172/1948-5956.1000009
- Anderson, G. R., Winter, P. S., Lin, K. H., Nussbaum, D. P., Cakir, M., Stein, E. M., et al. (2017). A landscape of therapeutic cooperativity in KRAS mutant cancers reveals principles for controlling tumor evolution. *Cell Rep.* 20, 999–1015. doi: 10.1016/j.celrep.2017.07.006
- Appel, C. K., Gallego-Pedersen, S., Andersen, L., Blanchefflor Kristensen, S., Ding, M., Falk, S., et al. (2017). The Src family kinase inhibitor dasatinib delays pain-related behaviour and conserves bone in a rat model of cancer-induced bone pain. *Sci. Rep.* 7:4792. doi: 10.1038/s41598-017-05029-1
- Araujo, J., and Logothetis, C. (2009). Targeting Src signaling in metastatic bone disease. *Int. J. Cancer* 124, 1–6. doi: 10.1002/ijc.23998
- Araujo, J., and Logothetis, C. (2010). Dasatinib: a potent SRC inhibitor in clinical development for the treatment of solid tumors. *Cancer Treat. Rev.* 36, 492–500. doi: 10.1016/j.ctrv.2010.02.015
- Araujo, J. C., Mathew, P., Armstrong, A. J., Braud, E. L., Posadas, E., Lonberg, M., et al. (2012). Dasatinib combined with docetaxel for castration-resistant prostate cancer: results from a phase 1-2 study. *Cancer* 118, 63–71. doi: 10.1002/cncr.26204
- Buglio, D., Palakurthi, S., Byth, K., Vega, F., Toader, D., Saeh, J., et al. (2012). Essential role of TAK1 in regulating mantle cell lymphoma survival. *Blood* 120, 347–355. doi: 10.1182/blood-2011-07-369397
- Carretero, J., Shimamura, T., Rikova, K., Jackson, A. L., Wilkerson, M. D., Borgman, C. L., et al. (2010). Integrative genomic and proteomic analyses identify targets for Lkb1-deficient metastatic lung tumors. *Cancer Cell* 17, 547–559. doi: 10.1016/j.ccr.2010.04.026
- Chen, J., Elfiky, A., Han, M., Chen, C., and Saif, M. W. (2014). The role of Src in colon cancer and its therapeutic implications. *Clin. Colorectal Cancer* 13, 5–13. doi: 10.1016/j.clcc.2013.10.003
- Copeland, R. A. (2013). *Evaluation of Enzyme Inhibitors In Drug Discovery: A Guide For Medicinal Chemists And Pharmacologists*. Hoboken, NJ: John Wiley & Sons.
- Cortes, J. E., Gambacorti-Passerini, C., Deininger, M. W., Mauro, M. J., Chuah, C., Kim, D. W., et al. (2019). Patient-reported outcomes in the phase 3 BFORE trial of bosutinib versus imatinib for newly diagnosed chronic phase chronic myeloid leukemia. *J. Cancer Res. Clin. Oncol.* 145, 1589–1599. doi: 10.1007/s00432-019-02894-3
- Daud, A. I., Krishnamurthi, S. S., Saleh, M. N., Gitlitz, B. J., Borad, M. J., Gold, P. J., et al. (2012). Phase I study of bosutinib, a src/abl tyrosine kinase inhibitor, administered to patients with advanced solid tumors. *Clin. Cancer Res.* 18, 1092–1100. doi: 10.1158/1078-0432.CCR-11-2378
- de Felice, M., Lambert, D., Holen, I., Escott, K. J., and Andrew, D. (2016). Effects of Src-kinase inhibition in cancer-induced bone pain. *Mol. Pain* 12, 1–14. doi: 10.1177/1744806916643725
- Du, G., Rao, S., Gurbani, D., Henning, N. J., Jiang, J., Che, J., et al. (2020). Structure-based design of a potent and selective covalent inhibitor for SRC kinase that targets a P-loop cysteine. *J. Med. Chem.* 63, 1624–1641. doi: 10.1021/acs.jmedchem.9b01502
- Duan, Y. Q., Ma, Y., Wang, X. J., Jin, Y. Y., Wang, R. L., Dong, W. L., et al. (2014). Design potential selective inhibitors for treating cancer by targeting the SRC homology 2 (SH2) domain-containing phosphatase 2 (Shp2) with core hopping approach. *Protein Pept. Lett.* 21, 556–563. doi: 10.2174/0929866521666131223143913
- Elias, D., and Ditzel, H. J. (2015). The potential of Src inhibitors. *Aging (Albany, NY)* 7, 734–735. doi: 10.18632/aging.100821
- Elkins, J. M., Fedele, V., Szklarz, M., Abdul Azeez, K. R., Salah, E., Mikolajczyk, J., et al. (2016). Comprehensive characterization of the published kinase inhibitor set. *Nat. Biotechnol.* 34, 95–103. doi: 10.1038/nbt.3374
- Emsley, P., and Cowtan, K. (2004). Coot: model-building tools for molecular graphics. *Acta Crystallogr. D Biol. Crystallogr.* 60(Pt 12 Pt 1), 2126–2132. doi: 10.1107/S0907444904019158
- Gierse, J. K., Koboldt, C. M., Walker, M. C., Seibert, K., and Isakson, P. C. (1999). Kinetic basis for selective inhibition of cyclo-oxygenases. *Biochem. J.* 339 (Pt 3), 607–614.
- Hiscox, S., Morgan, L., Green, T., and Nicholson, R. I. (2006). Src as a therapeutic target in anti-hormone/anti-growth factor-resistant breast cancer. *Endocr. Relat. Cancer* 13(Suppl. 1), S53–S59. doi: 10.1677/erc.1.01297
- Keskin, D., Sadri, S., and Eskazan, A. E. (2016). Dasatinib for the treatment of chronic myeloid leukemia: patient selection and special considerations. *Drug Des. Devel. Ther.* 10, 3355–3361. doi: 10.2147/DDDT.S85050
- Kwarcinski, F. E., Fox, C. C., Steffey, M. E., and Soellner, M. B. (2012). Irreversible inhibitors of c-Src kinase that target a nonconserved cysteine. *ACS Chem. Biol.* 7, 1910–1917. doi: 10.1021/cb300337u
- Lovly, C. M., and Shaw, A. T. (2014). Molecular pathways: resistance to kinase inhibitors and implications for therapeutic strategies. *Clin. Cancer Res.* 20, 2249–2256. doi: 10.1158/1078-0432.CCR-13-1610
- Marcotte, R., Smith, H. W., Sanguin-Gendreau, V., McDonough, R. V., and Muller, W. J. (2012). Mammary epithelial-specific disruption of c-Src impairs cell cycle progression and tumorigenesis. *Proc. Natl. Acad. Sci. U.S.A.* 109, 2808–2813. doi: 10.1073/pnas.1018861108
- McCoy, A. J., Grosse-Kunstleve, R. W., Adams, P. D., Winn, M. D., Storoni, L. C., and Read, R. J. (2007). Phaser crystallographic software. *J. Appl. Crystallogr.* 40(Pt 4), 658–674. doi: 10.1107/S0021889807021206
- McDonnell, D. P., and Norris, J. D. (2002). Connections and regulation of the human estrogen receptor. *Science* 296, 1642–1644. doi: 10.1126/science.1071884
- McMillan, E. A., Ryu, M. J., Diep, C. H., Mendiratta, S., Clemenceau, J. R., Vaden, R. M., et al. (2018). Chemistry-first approach for nomination of personalized treatment in lung cancer. *Cell* 173, 864–878. doi: 10.1016/j.cell.2018.03.028
- Minor, W., Cymborowski, M., Otwinowski, Z., and Chruszcz, M. (2006). HKL-3000: the integration of data reduction and structure solution—from diffraction images to an initial model in minutes. *Acta Crystallogr. D Biol. Crystallogr.* 62(Pt 8), 859–866. doi: 10.1107/S0907444906019949
- Miyahisa, I., Sameshima, T., and Hixon, M. S. (2015). Rapid determination of the specificity constant of irreversible inhibitors (kinact/KI) by means of an endpoint competition assay. *Angew. Chem. Int. Ed. Engl.* 54, 14099–14102. doi: 10.1002/anie.201505800

- Papp-Wallace, K. M., Mallo, S., Bethel, C. R., Taracila, M. A., Hujer, A. M., Fernandez, A., et al. (2014). A kinetic analysis of the inhibition of FOX-4 beta-lactamase, a plasmid-mediated AmpC cephalosporinase, by monocyclic beta-lactams and carbapenems. *J. Antimicrob. Chemother.* 69, 682–690. doi: 10.1093/jac/dkt434
- Park, K. S., Raffeld, M., Moon, Y. W., Xi, L., Bianco, C., Pham, T., et al. (2014). CRIPTO1 expression in EGFR-mutant NSCLC elicits intrinsic EGFR-inhibitor resistance. *J. Clin. Invest.* 124, 3003–3015. doi: 10.1172/JCI73048
- Puls, L. N., Eadens, M., and Messersmith, W. (2011). Current status of SRC inhibitors in solid tumor malignancies. *Oncologist* 16, 566–578. doi: 10.1634/theoncologist.2010-0408
- Rao, S., Gurbani, D., Du, G. Y., Everley, R. A., Browne, C. M., Chaikuad, A., et al. (2019). Leveraging compound promiscuity to identify targetable cysteines within the kinome. *Cell Chem. Biol.* 26, 818–829. doi: 10.1016/j.chembiol.2019.02.021
- Schott, A. F., Barlow, W. E., Van Poznak, C. H., Hayes, D. F., Moinpour, C. M., Lew, D. L., et al. (2016). Phase II studies of two different schedules of dasatinib in bone metastasis predominant metastatic breast cancer: SWOG S0622. *Breast Cancer Res. Treat.* 159, 87–95. doi: 10.1007/s10549-016-3911-z
- Schwartz, P. A., Kuzmic, P., Solowiej, J., Bergqvist, S., Bolanos, B., Almaden, C., et al. (2014). Covalent EGFR inhibitor analysis reveals importance of reversible interactions to potency and mechanisms of drug resistance. *Proc. Natl. Acad. Sci. U.S.A.* 111, 173–178. doi: 10.1073/pnas.1313733111
- Secord, A. A., Teoh, D. K., Barry, W. T., Yu, M., Broadwater, G., Havrilesky, L. J., et al. (2012). A phase I trial of dasatinib, an SRC-family kinase inhibitor, in combination with paclitaxel and carboplatin in patients with advanced or recurrent ovarian cancer. *Clin. Cancer Res.* 18, 5489–5498. doi: 10.1158/1078-0432.CCR-12-0507
- Sen, B., and Johnson, F. M. (2011). Regulation of SRC family kinases in human cancers. *J. Signal Transduct.* 2011:865819. doi: 10.1155/2011/865819
- Sen, B., Peng, S., Saigal, B., Williams, M. D., and Johnson, F. M. (2011). Distinct interactions between c-Src and c-Met in mediating resistance to c-Src inhibition in head and neck cancer. *Clin. Cancer Res.* 17, 514–524. doi: 10.1158/1078-0432.CCR-10-1617
- Shah, N. P., Kim, D. W., Kantarjian, H., Rousselot, P., Llacer, P. E., Enrico, A., et al. (2010). Potent, transient inhibition of BCR-ABL with dasatinib 100 mg daily achieves rapid and durable cytogenetic responses and high transformation-free survival rates in chronic phase chronic myeloid leukemia patients with resistance, suboptimal response or intolerance to imatinib. *Haematologica* 95, 232–240. doi: 10.3324/haematol.2009.011452
- Sharma, M. R., Wroblewski, K., Polite, B. N., Knost, J. A., Wallace, J. A., Modi, S., et al. (2012). Dasatinib in previously treated metastatic colorectal cancer: a phase II trial of the University of Chicago phase II consortium. *Invest. New Drugs* 30, 1211–1215. doi: 10.1007/s10637-011-9681-x
- Stehelin, D., Varmus, H. E., Bishop, J. M., and Vogt, P. K. (1976). DNA related to the transforming gene (s) of avian sarcoma viruses is present in normal avian DNA. *Nature* 260, 170–173.
- Tan, L., Gurbani, D., Weisberg, E. L., Hunter, J. C., Li, L., Jones, D. S., et al. (2017). Structure-guided development of covalent TAK1 inhibitors. *Bioorg. Med. Chem.* 25, 838–846. doi: 10.1016/j.bmc.2016.11.035
- Trevino, J. G., Summy, J. M., Lesslie, D. P., Parikh, N. U., Hong, D. S., Lee, F. Y., et al. (2006). Inhibition of SRC expression and activity inhibits tumor progression and metastasis of human pancreatic adenocarcinoma cells in an orthotopic nude mouse model. *Am. J. Pathol.* 168, 962–972. doi: 10.2353/ajpath.2006.050570
- Wu, Z.-H., Lin, C., Liu, M.-M., Zhang, J., Tao, Z.-H., and Hu, X.-C. (2016). Src inhibition can synergize with gemcitabine and reverse resistance in triple negative breast cancer cells via the AKT/c-jun pathway. *PLoS ONE* 11:e0169230. doi: 10.1371/journal.pone.0169230
- Winn, M. D., Ballard, C. C., Cowtan, K. D., Dodson, E. J., Emsley, P., Evans, P. R., et al. (2011). Overview of the CCP4 suite and current developments. *Acta Crystallogr. D Biol. Crystallogr.* (2011) 67, 235–242. doi: 10.1107/S0907444910045749
- Zhang, X. H., Wang, Q., Gerald, W., Hudis, C. A., Norton, L., Smid, M., et al. (2009). Latent bone metastasis in breast cancer tied to Src-dependent survival signals. *Cancer Cell* 16, 67–78. doi: 10.1016/j.ccr.2009.05.017

Conflict of Interest: KW is on the SAB for Vibriome Therapeutics. NG is a founder, SAB, and equity holder in Gatekeeper, Syros, Petra, C4, B2S, and Soltego. The Gray lab receives/has received funding from Novartis, Takeda, Astellas, Taiho, Janssen, Kinogen, Voronoi, Her2llc, Deerfield, and Sanofi. GD, NH, SR, DG, TZ, KW, and NG are inventors on a Src covalent inhibitor patent. Information regarding Src is accessible via UniProtKB P12931.

The remaining author declares that the research was conducted in the absence of any commercial or financial relationships that could be construed as a potential conflict of interest.

Copyright © 2020 Gurbani, Du, Henning, Rao, Bera, Zhang, Gray and Westover. This is an open-access article distributed under the terms of the Creative Commons Attribution License (CC BY). The use, distribution or reproduction in other forums is permitted, provided the original author(s) and the copyright owner(s) are credited and that the original publication in this journal is cited, in accordance with accepted academic practice. No use, distribution or reproduction is permitted which does not comply with these terms.

KEY RESOURCES TABLE

Reagent or resource	Source	Identifier
BACTERIAL STRAINS		
<i>E. coli</i> BL21DE3 cells	Gift from Dr. M. Seeliger (SUNY, Stony Brook)	N/A
Src kinase purification, assays, and crystal structure	Gift from Dr. M. Seeliger (SUNY, Stony Brook)	N/A
pET28a Src kinase expression vector		
Custom oligos: AAGCTGGGGCAGGGCAGCTTTGGAGAGGTCTGG	Sigma-Aldrich	N/A
QuikChange II Site-Directed Mutagenesis Kit	Agilent Technologies	Cat # 200524
Kanamycin	Sigma-Aldrich	Cat # K1377
Streptomycin	Sigma-Aldrich	Cat # S9137
Chloramphenicol	Sigma-Aldrich	Cat # C0378
Bosutinib	Sigma-Aldrich	Cat # PZ0192
SM1-71	Prof. Nathanael Gray, DFCL, Harvard	https://graylab.dana-farber.org/
DGY-06-116	Prof. Nathanael Gray, DFCL, Harvard	https://graylab.dana-farber.org/
NJH-01-111	Prof. Nathanael Gray, DFCL, Harvard	https://graylab.dana-farber.org/
LabChip® EZ Reader automated microcapillary electrophoresis platform	PerkinElmer	https://www.perkinelmer.com/product/assy-ez-reader-ii-ship-level-122919
Fluorescently labeled peptide-4 substrate	Perkin Elmer	https://www.perkinelmer.com/product/dkp-peptide-4-packed-760348
EZ-Link™ Sulfo-NHS-Biotinylation Kit	ThermoFisher	Cat # 21425
Biacore S200	GE Healthcare	https://www.gelifesciences.com/en/us/shop/protein-analysis/spr-label-free-analysis/systems/biacore-s200-p-05541
Biotin Capture Kit and Sensor Chip CAP	GE Healthcare	Cat # 28920233
Deposited data Src-DGY-06-116	https://www.rcsb.org/thisstudy	PDB ID: 6E6E
SOFTWARE AND ALGORITHMS		
EZReader 3.0 software	Perkin Elmer	https://www.perkinelmer.com/lab-products-and-services/resources/software-downloads.html
GraphPad software version 7	GraphPad Software	www.graphpad.com
HKL3000	(Minor et al., 2006)	https://sbgrid.org/
PHENIX 1.14rc3_319	(Adams et al., 2010)	https://sbgrid.org/
Coot	Emsley and Cowtan, 2004	https://sbgrid.org/
CCP4 7.0	Winn et al., 2011	https://sbgrid.org/
Pymol 2.3	Schrodinger, LLC	https://sbgrid.org/
LIGPLOT	Laskowski R A, Swindells M B (2011)	https://www.ebi.ac.uk/thornton-srv/software/LigPlus/
Biacore™ insight evaluation software	GE Healthcare Life Sciences, USA.	https://www.gelifesciences.com/en/us/shop/protein-analysis/spr-label-free-analysis/systems/biacore-s200-p-05541

METHOD DETAILS

Expression, Purification and Crystallization of Human Src Kinase and Cys₂₈₀-Ser Mutant Src Kinase

The Src (UniProtKB P12931) kinase domain was purified as reported previously (Rao et al., 2019). The Cys₂₈₀-Ser mutant

Src version was generated via site-directed mutagenesis and purified similarly.

Enzymatic Assay for IC₅₀ Determination

An automated microcapillary electrophoresis platform (PerkinElmer LabChip® EZ Reader) capable of separating and detecting fluorescently labeled peptides based on charge

(Elkins et al., 2016) was used for measuring Src kinase activity. Briefly, purified Src enzyme, fluorescently labeled peptide-4 substrate (purchased from Perkin Elmer), ATP, and inhibitors (SM1-71, Bosutinib, DGY-06-116, and NJH-01-111) were combined into a single well, incubated for 1 h incubation following phosphorylation of the substrate. Substrate (non-phosphorylated peptide) to product (phosphorylated peptide as a result of Src kinase activity) conversion was measured over time. The kinase reaction buffer consisted of 100 mM Hepes, pH 7.3, 0.015% Brij-35, 0.004% Tween-20, and 10 mM MgCl₂. Peptides were separated using running buffer made of 100 mM Hepes, pH 7.3, 0.015% Brij-35, 1 mM disodium EDTA, 0.1% coating reagent 3, 5% DMSO, and 1× coating reagent 8. Final reaction conditions included 1.25 nM of purified Src kinase, 100 μM ATP, and 1 μM peptide-4 substrate. The percent conversion was determined by EZReader 3.0 software and analyzed using GraphPad software version 7 (La Jolla, California, USA) for determination of IC₅₀ values.

Crystallization and Structure

Determination of Src-DGY-06-116 Complex

Purified Src kinase was concentrated to 10 mg/ml and incubated with three fold excess of inhibitor DGY-06-116 at room temperature for 1 h. Co-crystals of Src-DGY-06-116 complex were obtained by vapor diffusion from a hanging drop setup at 20 Å°C using 0.1 M magnesium formate dihydrate and 15% PEG3350 as precipitant. Crystals appeared overnight and were harvested after 2 days in mother liquor with 30% glycerol before freezing in liquid nitrogen. Diffraction data were collected using beamline 19-ID of the Advanced Photon Source, Argonne

National Laboratory and scaled using HKL3000 (Minor et al., 2006). Molecular replacement solution was obtained using Phaser (McCoy et al., 2007) and 4MXO as initial search model. Model building and refinement were carried out using Coot (Emsley and Cowtan, 2004) and Phenix (Adams et al., 2010).

SPR Based Kinetics of Covalent Inhibition

A Biacore S200 was used to evaluate binding of covalent inhibitor DGY-06-116 and its non-covalent analog NJH-01-111 with Src kinase. Src was biotinylated using EZ-Link™ Sulfo-NHS-Biotinylation Kit (ThermoFisher). Biotinylated Src kinase was captured using the Biotin Capture Kit and Sensor Chip CAP (GE Healthcare). The Biotin Capture Kit works with a single-stranded DNA sequence on Sensor Chip CAP. A capture reagent consisting of a biotinylated complementary DNA strand and streptavidin is captured by the single-stranded DNA, allowing capture of other biotinylated molecules by streptavidin. At the end of the binding cycle, the DNA duplex is chemically disrupted, washing away all materials except the original single-stranded DNA sequence. The sequence is repeated for each binding cycle of the assay. Src was captured at surface densities between 800 and 900 RU for each cycle of the assay. Dilutions of DGY-06-116 and NJH-01-111 from 100 to 1.2 nM were made in running buffer (100 mM HEPES pH 7.3, 0.015% Brij-35, 0.004% Tween-20, 10 mM MgCl₂, and 1% DMSO) and tested for binding using a multi-cycle assay. The SPR data were analyzed using Biacore™ Insight Evaluation Software (GE Healthcare Life Sciences, USA). Data from each interaction were analyzed using both a 1:1 kinetic model and a two-state covalent interaction model (involving p-loop movement) for calculation of $k_{\text{inact}}/K_{\text{I}}$ using Biacore S200 Evaluation software (GE Healthcare Life Sciences, USA).